JMEPEG
https://doi.org/10.1007/s11665-020-04826-6

Low Young's Modulus and High Strength Obtained in Ti-Nb-Zr-Cr Alloys by Optimizing Zr Content

Qiang Li, Chao Cheng, Junjie Li, Ke Zhang, Kai Zhou, Masaaki Nakai, Mitsuo Niinomi, Kenta Yamanaka, Daixiu Wei, Akihiko Chiba, and Takayoshi Nakano

(Submitted January 22, 2020; in revised form April 1, 2020)

A series of Ti-29Nb-(4, 7, 10, 13)Zr-2Cr alloys were fabricated to investigate the influence of Zr content on microstructures and mechanical properties. All the four alloys present a single β phase after solution treatment. With the increase in Zr content, the 0.2% proof stress is gradually increased from 388 MPa in Ti-29Nb-4Zr-2Cr to 713 MPa in Ti-29Nb-13Zr-2Cr. The Young's modulus gradually is decreased from 80 GPa in Ti-29Nb-4Zr-2Cr to 63 GPa in Ti-29Nb-13Zr-2Cr. The elongation shows the same trend as that of Young's modulus. The changes of mechanical properties are influenced by the β stability and solid solution strengthening effect, which are both enhanced by Zr addition. The Ti-29Nb-13Zr-2Cr alloy presents a Young's modulus of 63 GPa, tensile strength of 730 MPa and elongation of 18% and is a promising biomedical material.

Keywords β-type Ti alloys, biomaterial, mechanical properties, microstructure

1. Introduction

Ti and Ti alloys are widely used as biomaterials owing to the good mechanical properties, excellent corrosion resistance and desirable biocompatibility (Ref 1). Although commercially pure Ti (C.P.-Ti) is used in some orthopedic and dental fields, the low strength and low wear resistance limits its application as biomaterial (Ref 2). The Ti-6Al-4V alloy, which is developed for the aerospace industry, shows improved mechanical properties (Ref 2, 3). However, Al and V may lead to long-term health problems, which cause people's concerns about the safety of the material (Ref 4). Additionally, the Young's moduli of C.P.-Ti and Ti-6Al-4V are much higher than that of human bone (10-30 GPa). The applied load is mostly carried by the implants rather than the bone, which causes stress shielding effect and results in bone atrophies (Ref 4, 5). Therefore, current researches focus on developing low Young's modulus β-type Ti alloys composed of non-toxic elements including Nb, Zr, Ta, Sn and so on. (Ref 6, 7).

Nb is the mostly used β stabilizer to design biomedical β-type Ti alloys because Ti-Nb-based alloys always perform low Young's modulus (Ref 7). Zr and Ti are of the same family and have similar physical and chemical properties. Although Zr is a so-called neutral element, it can reduce M_s (martensitic transformation starting temperature) point and so works as a weak β stabilizer in some β-type Ti alloys (Ref 8). A large number of Ti-Nb-Zr-based alloys are designed such as Ti-13Nb-13Zr (wt.%) (Ref 9), Ti-22Nb-6Zr (at.%) (Ref 10), Ti-28Nb-35.4Zr (wt.%) (Ref 11), Ti-24Nb-2Zr (at.%) (Ref 12). Cr is an effective β stabilizer. Ti-Cr binary alloys are demonstrated non-toxic to cells, thus Cr is suitable to add in biomedical Ti alloys and many alloys have been studied including Ti-27Nb-7Fe-8Cr (wt.%) (Ref 13), Ti-15Mo-6Zr-2Cr (wt.%) (Ref 14), Ti-12Cr (wt.%) (Ref 15), Ti-22Nb-2Cr (wt.%) (Ref 16) and Ti-33Zr-7Fe-4Cr (wt.%) (Ref 17). Improved mechanical properties can be obtained by optimizing fabricating methods, heat treatments and surface modifications. The tensile strength, fatigue property and super-elasticity can be increased by ω phase precipitation after aging treatment (Ref 12, 18). Ti-35Nb-2Ta-3Zr fabricated by selective laser sintering (SLS) exhibits significantly improved super-elastic recoverable strain up to

Qiang Li, Chao Cheng, and **Kai Zhou**, School of Mechanical Engineering, University of Shanghai for Science and Technology, Shanghai 200093, People's Republic of China; **Junjie Li**, CAS Key Laboratory of Functional Materials and Devices for Special Environments, Xinjiang Technical Institute of Physics and Chemistry, CAS, Xinjiang Key Laboratory of Electronic Information Materials and Devices, 40-1 South Beijing Road, Urumqi 830011, China; **Ke Zhang**, School of Materials Science and Engineering, University of Shanghai for Science and Technology, Shanghai 200093, People's Republic of China; **Masaaki Nakai**, Department of Mechanical Engineering, Faculty of Science and Engineering, Kindai University, 3–4–1 Kowakae, Higashiosaka, Osaka 577–8502, Japan; **Mitsuo Niinomi**, School of Mechanical Engineering, University of Shanghai for Science and Technology, Shanghai 200093, People's Republic of China; Institute for Materials Research, Tohoku University, 2–1–1, Katahira, Aoba-ku, Sendai 980–5377, Japan; Department of Materials and Manufacturing Science, Graduate School of Engineering, Osaka University, 2–1, Yamada-Oka, Suita, Osaka 565–0871, Japan; Department of Materials Science and Engineering, Graduate School of Science and Technology, Meijo University, 1–501, Shiogamaguchi, Tempaku-ku, Nagoya 468–8502, Japan; Institute of Materials and Systems for Sustainability, Nagoya University, Furo-cho, Chikusa-ku, Nagoya 464–8601, Japan; and Faculty of Chemistry, Materials and Bioengineering, Kansai University, Osaka 564–860, Japan; **Kenta Yamanaka, Daixiu Wei,** and **Akihiko Chiba**, Institute for Materials Research, Tohoku University, 2–1–1, Katahira, Aoba-ku, Sendai 980–5377, Japan; **Takayoshi Nakano**, Department of Materials and Manufacturing Science, Graduate School of Engineering, Osaka University, 2–1, Yamada-Oka, Suita, Osaka 565–0871, Japan. Contact e-mails: jxli@tju.edu.cn, liqiang@usst.edu.cn, and niinomi@imr.tohoku.ac.jp.

Published online: 07 May 2020

4.8% (Ref 19). The nitrided, oxynitrided and carbonitrided layers prepared by thermal spraying and plasma deposition can enhance the corrosion resistance, biocompatibility, wear resistance and fatigue limit (Ref 20-22). The Ti alloys subjected to shot peening, surface mechanical attrition treatment and friction stir processing show improved wear resistance, fatigue property and super-elasticity owing to the severe deformation layer or nanocrystalline layer on the surface (Ref 23-25).

Among all the novel β-type Ti alloys, Ti-29Nb-13Ta-4.6Zr is one of the most well-known β-type Ti alloys designed for biomedical application (Ref 26). It shows a low Young's modulus of 55 GPa, which is very near to bone (Ref 4). Animal tests prove that the stress transfer between the bone and the implant is uniform, thus good bone remodeling is achieved in Ti-29Nb-13Ta-4.6Zr (Ref 27, 28). In order to further reduce the cost, Ta with high melting point and high cost is supposed to be replaced by Cr. In order to obtain similar β phase stability in the alloy with the Nb content unchanged, 13% Ta is substituted by 2% Cr based on the calculation of Mo equivalent (Ref 29). It is expected that the designed alloys can also perform low Young's modulus. The β phase stability is slightly adjusted to obtain good mechanical properties by changing Zr content. Therefore, Ti-29Nb-(4, 7, 10, 13)Zr-2Cr alloys are designed and the microstructures and mechanical properties are investigated in this study.

2. Experimental Procedures

The ingots of Ti-29Nb-(4, 7, 10, 13)Zr-2Cr (wt.%, hereafter, chemical compositions of present alloys are in wt.%) were arc-melted in a water-cooled copper crucible in Ar atmosphere. The ingots were homogenized at 1273 K for 36 ks and then solution-treated at 1123 K for 3.6 ks followed by water quenching. They were cold-rolled to sheets with a final thickness of 1.5 mm under a total reduction ratio of 85% at room temperature without intermediate annealing. The sheets were solution-treated at 1073 K for 3.6 ks followed by water quenching.

The samples for microstructural observation were mechanically ground by SiC waterproof paper, mirror-polished by SiO_2 suspension and then etched in a 5-vol.% HF solution for approximately 15 s. The phases were analyzed by a Bruker D8 x-ray diffractometer (XRD) with Cu-Kα radiation at a voltage of 40 kV and current of 40 mA. The specimens for tensile test and Young's modulus measurement were cut by wire electric discharge machining. Tensile tests were carried out under a crosshead speed of 0.5 mm/min at room temperature using the specimens with gage part of 12 mm × 3 mm × 1.5 mm. The specimens with size of 40 mm × 10 mm × 1.5 mm were subjected to free resonance vibration method at room temperature to measure the Young's moduli of the alloys. The transverse bending vibration of the sample was made by the excitation signal through the excitation sensor. The resonance frequency of the sample was measured by the pickup sensor. The dynamic Young's modulus (E) was calculated using the expression (Ref 30)

$$E = 0.9694\frac{mL^3f_r^2}{wd^3} \qquad \text{(Eq 1)}$$

where m, L, w and d were the weight, length, width and thickness of specimens, respectively; f_r was the intrinsic resonance vibration frequency.

3. Results

3.1 XRD Results

All the solution-treated alloys are composed of single β phase according to XRD patterns as shown in Fig. 1. Diffraction peak corresponding to the α'' phase or any other phase is not observed from the XRD patterns of the alloys, which means that the M_s temperature of these alloys is lower than room temperature. It is noticed that the peak position of $(110)_\beta$ gradually shifts to the left with the increase in Zr content. The calculated lattice parameter "a" values based on $(110)_\beta$ diffraction peak for Ti-29Nb-(4, 7, 10, 13)Zr-2Cr are 0.3800, 0.3812, 0.3823 and 0.3833 nm, respectively. The lattice parameter is increased by adding Zr, because the atomic radius of Zr (0.160 nm) is higher than those of Nb (0.147 nm) and Ti (0.145 nm) (Ref 31).

Figure 2 presents the XRD patterns of Ti-Nb-Zr-Cr alloys after tensile tests. The change of the peaks is hardly found in Fig. 2 comparing with Fig. 1. The deformed specimens also show single β phase according to XRD patterns. There are two possibilities occurring in tensile tests. If there is no stress-induced α'' martensite transformation during tension, there will be no change found in XRD patterns. If the α'' phase is stress-induced during loading and almost fully reverses to β phase after fracture, the change of phase will also not be detected by XRD in the deformed specimens. The deformation behaviors are further analyzed by microstructural observation and tensile curves. More details about the deformation behavior are discussed in the following sections.

3.2 Microstructures

As shown in Fig. 3, only equiaxed β grains can be observed in Ti-29Nb-(4, 7, 10, 13)Zr-2Cr alloys after solution treatment. There is no α'' martensite or any other phase existing in the β grains, which is consistent with the XRD results. The average grain size gradually decreases from ~ 94 μm in Ti-29Nb-4Zr-2Cr to ~ 40 μm in Ti-29Nb-13Zr-2Cr. It shows that Zr plays a role on the grain refinement, which is also reported in Ti-35Nb-(2, 4, 6, 8)Zr ternary alloys (Ref 32).

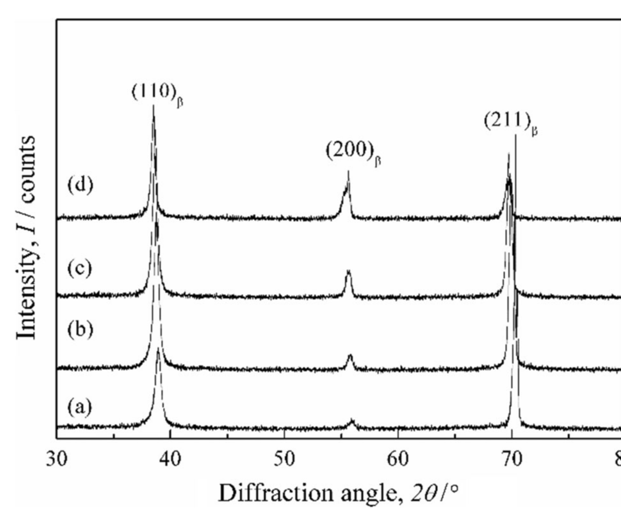

Fig. 1 XRD patterns of Ti-Nb-Zr-Cr alloys subjected to solution treatments: (a) Ti-29Nb-4Zr-2Cr, (b) Ti-29Nb-7Zr-2Cr, (c) Ti-29Nb-10Zr-2Cr and (d) Ti-29Nb-13Zr-2Cr

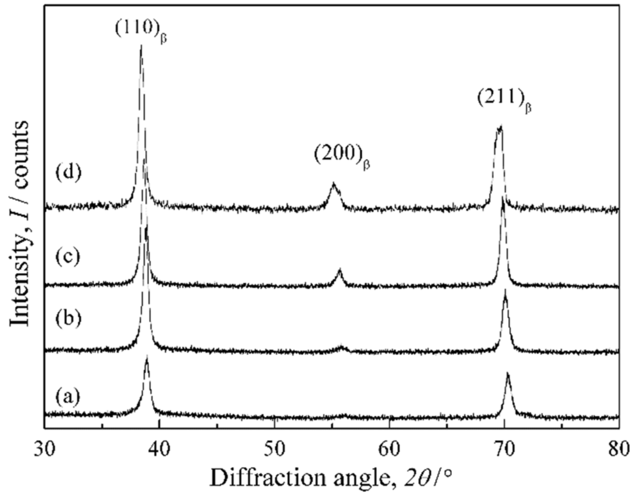

Fig. 2 XRD patterns of Ti-Nb-Zr-Cr alloys after tensile tests: (a) Ti-29Nb-4Zr-2Cr, (b) Ti-29Nb-7Zr-2Cr, (c) Ti-29Nb-10Zr-2Cr and (d) Ti-29Nb-13Zr-2Cr

After tensile test, a lot of deformation bands can be observed in the β grains of Ti-29Nb-4Zr-2Cr, as shown in Fig. 4(a). The deformation bands are decreased with the increase in Zr content (Fig. 4b and c) and disappear in Ti-29Nb-13Zr-2Cr (Fig. 4d). Metastable β-type Ti alloys have multiple deformation mechanisms, such as $\{332\}_\beta\langle113\rangle_\beta$ twinning, $\{112\}_\beta\langle111\rangle_\beta$ twinning, stress-induced α'' martensite transformation and deformation-induced ω phase transformation (Ref 33). The $\{112\}_\beta\langle111\rangle_\beta$ twinning is a well-known twinning mode formed in bcc metals and alloys. The lattice instability of the metastable β phase allows complex movement of atoms and makes $\{332\}_\beta\langle113\rangle_\beta$ twinning possible (Ref 34). Additionally, the reverse $\alpha'' \rightarrow \beta$ transformation is involved in the formation of $\{332\}_\beta\langle113\rangle_\beta$ in Ti-40Nb (wt.%) and Ti-14Mo (wt.%), which exhibit stress-induced α'' martensite transformation during tension (Ref 35, 36). The $\{332\}_\beta\langle113\rangle_\beta$ twinning is also found in metastable β-type Ti alloys including Ti-24Nb-2Zr (at.%), Ti-14.8V (wt.%), Ti-10Mo-1Fe (wt.%), Ti-14Nb-2Fe (at.%), Ti-36Nb-2Ta-3Zr (wt.%) and Ti-15Mo(wt.%) (Ref 12, 29, 37-40). It is believed that the twinning possibly forms in metastable β-type Ti alloys with Mo equivalent values between 9.9 and 15. Since the Zr content is not considered in calculating Mo equivalent value, the Mo equivalent values of Ti-29Nb-(4, 7, 10, 13)Zr-2Cr are all 10.62. The microstructures in Fig. 4(a), (b) and (c) are similar with the microstructures of deformed Ti-(14, 16, 18)Nb-2Fe (at.%) alloys (Ref 38); thus, the deformation bands can be viewed as twinning. Although the Mo equivalent value is not changed by Zr content, adding Zr increases the β stability of the alloy. Thus, the deformation bands are decreased with the Zr contents increased from 4 to 10% and disappear in Ti-29Nb-13Zr-2Cr.

3.3 Mechanical Properties

Figure 5 presents the true stress–strain curves of Ti-Nb-Zr-Cr alloys obtained by tensile tests at room temperature. Ti-29Nb-(4, 7, 10)Zr-2Cr with metastable β phase do not show a clear yielding phenomenon due to the unstable β phase and stress-induced α'' martensite transformation (Ref 41). As above mentioned, residual α'' phase is hardly found in the XRD patterns and microstructures. The reason is that the A_f temperatures (so-called austenite finishing temperature at which the reverse α'' to β martensitic transformation completes after unloading) of the alloys are lower than room temperature and the stress-induced α'' martensite can reverse to β phase after

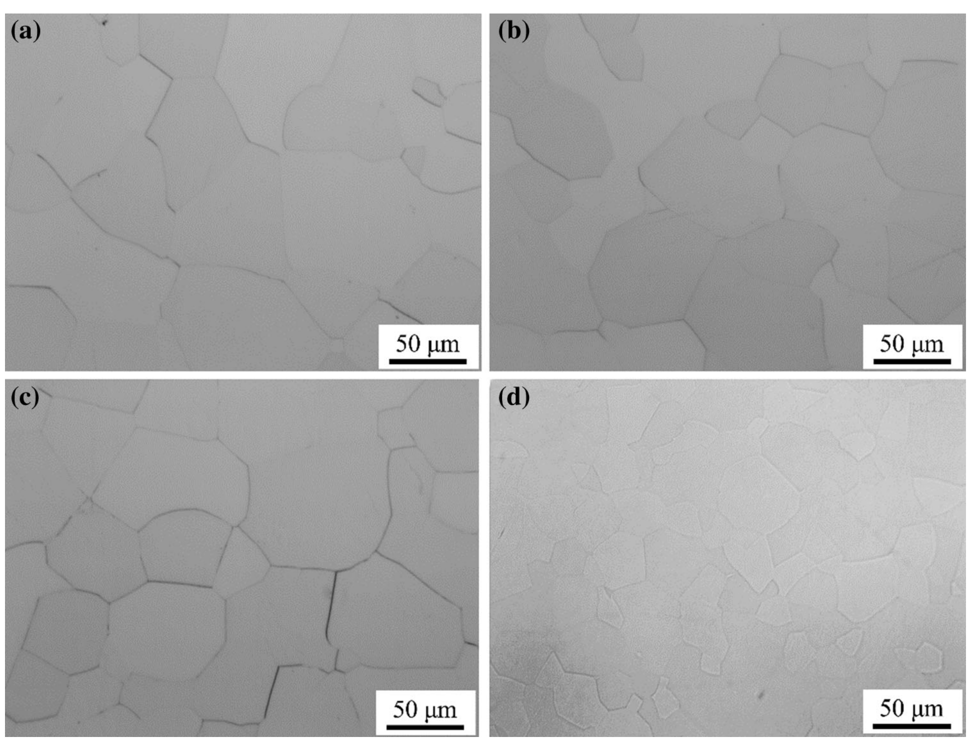

Fig. 3 Microstructures of Ti-Nb-Zr-Cr alloys subjected to solution treatments: (a) Ti-29Nb-4Zr-2Cr, (b) Ti-29Nb-7Zr-2Cr, (c) Ti-29Nb-10Zr-2Cr and (d) Ti-29Nb-13Zr-2Cr

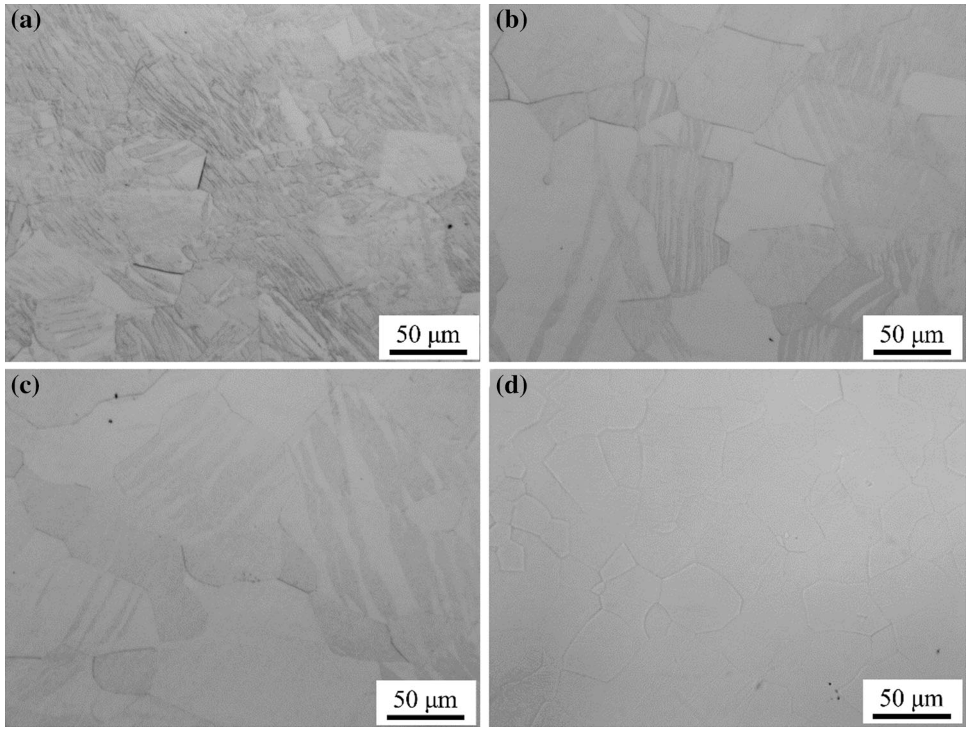

Fig. 4 Microstructures of Ti-Nb-Zr-Cr alloys after tensile tests: (a) Ti-29Nb-4Zr-2Cr, (b) Ti-29Nb-7Zr-2Cr, (c) Ti-29Nb-10Zr-2Cr and (d) Ti-29Nb-13Zr-2Cr

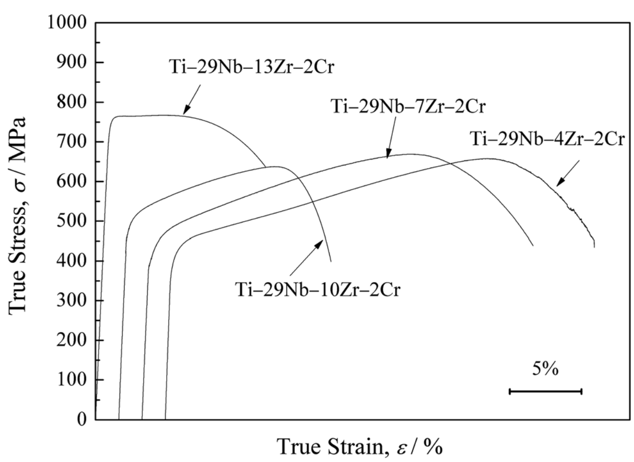

Fig. 5 True stress–strain curves of Ti-Nb-Zr-Cr alloys obtained by tensile tests

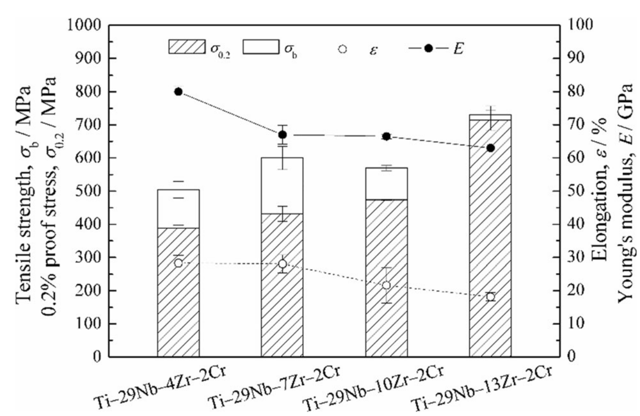

Fig. 6 Mechanical properties measured by tensile tests and Young's modulus obtained by free resonance vibration method

fracture. The Ti-29Nb-13Zr-2Cr shows a little obvious yield deformation indicating more stable β phase.

In the true stress–strain curves, the stress of Ti-29Nb-(4, 7, 10)Zr-2Cr increases significantly with the increase in strain in the plastic deformation stage, showing a strong work hardening behavior. It is because that during deformation, Ti-29Nb-(4, 7, 10)Zr-2Cr process twinning, which have been pointed out to cause high work hardening effect in metastable β-Ti alloys (Ref 37, 42). Ti-29Nb-13Zr-2Cr without twinning shows a nearly platform of stress after yielding until break, indicating a weak work hardening behavior.

Figure 6 shows tensile strength (σ_b), 0.2% proof stress ($\sigma_{0.2}$) and elongation (ε) measured by tensile tests, and Young's modulus obtained by free resonance vibration method. With the increase in Zr content, the Young's modulus is gradually decreased from 80 GPa in Ti-29Nb-4Zr-2Cr to 63 GPa in Ti-29Nb-13Zr-2Cr. The change in Young's modulus is mainly caused by two factors. The first factor is the enhanced β stability with the increase in Zr content. The lowest Young's modulus is usually obtained in the transition region for the β phase shifting from metastable state to stable state (Ref 43). The second factor is that the mean bond order $\overline{B_o}$ values of the alloys, which is calculated by:

$$\overline{B}_o = \sum_{i=1}^{n} X_i (B_o)_i \qquad \text{(Eq 2)}$$

where x_i is the atomic percentage of element i in the alloy and $(Bo)_i$ is the bond order for element i, which is related to strength of the covalent bonding between Ti and an alloying element (Ref 29, 44). The $\overline{B_o}$ values of Ti-29Nb-(4, 7, 10, 13)Zr-2Cr are 2.852, 2.859, 2.866 and 2.873, respectively, presenting an increasing trend with increase in Zr. It is reported that the higher $\overline{B_o}$ value causes lower Young's modulus in β-type Ti alloys (Ref 43). Therefore, the Young's modulus shows a downtrend as the Zr content is increased from 4 to 13%. The Young's modulus of 63 GPa in Ti-29Nb-13Zr-2Cr alloy is much lower than those of C.P.-Ti, Ti-6Al-4V and Ti-15Mo (Ref 45) and similar as some well-known β-type Ti alloys, such as Ti-29Nb-13Ta-4.6Zr (referred to as TNTZ) (Ref 26), Ti-24Nb-4Zr-7.9Sn (referred to as Ti-2448) (Ref 46) and Ti-35Nb-7Zr-5Ta (referred to as TNZT) (Ref 47).

The elongation shows the same trend as that of Young's modulus. However, the elongation is closely related to the microstructure and deformation mechanism of the alloys. Twinning-induced plasticity (TWIP) and transformation-induced plasticity (TRIP) are reported in some metastable β-type Ti alloy (Ref 42, 48, 49). The Ti-29Nb-(4, 7)Zr-2Cr alloys with TWIP and TRIP show large elongation around 28%. With the Zr content increased from 7 to 13%, the twinning and stress-induced martensite transformation are inhibited with the increase of β stability. Ti-29Nb-10Zr-2Cr and Ti-29Nb-13Zr-2Cr show lower elongations, which are 22 and 18%, respectively.

The $\sigma_{0.2}$ corresponds to the stress in the early stage of plastic deformation. With the increase in Zr and decrease in grain size, the $\sigma_{0.2}$ is increased from 388 MPa in Ti-29Nb-4Zr-2Cr to 713 MPa in Ti-29Nb-13Zr-2Cr. The increase of $\sigma_{0.2}$ confirms the solution strengthening effect of Hume–Rothery principle (Ref 50, 51) and fine grain strengthening effect of Hall–Petch formula (Ref 51, 52). In addition, Fleischer also proved that $\sigma_{0.2}$ is related to the concentration of solute atoms, and C in the formula of $\sigma \approx C^{2/3}$ is the content of solute elements in the alloy (Ref 50). The solute elements Zr and Cr in the alloys are helpful to obtain a higher $\sigma_{0.2}$. It is supposed that the σ_b should also be continuously increased by Zr addition. However, an abnormal phenomenon is found in Ti-29Nb-7Zr-2Cr and Ti-29Nb-10Zr-2Cr. Ti-29Nb-10Zr-2Cr shows lower σ_b than that of Ti-29Nb-7Zr-2Cr. According to the stress–strain curves, if the strain is the same, Ti-29Nb-10Zr-2Cr performs higher stress than that of Ti-29Nb-7Zr-2Cr, which is agreed with the hardening effect cause by Zr. However, Ti-29Nb-10Zr-2Cr fractures much earlier than Ti-29Nb-7Zr-2Cr. The poorer plasticity of the Ti-29Nb-10Zr-2Cr limits the hardening effect and results in lower σ_b. Although the elongation of Ti-29Nb-13Zr-2Cr with stable β phase is further decreased, it shows the highest $\sigma_{0.2}$ of 713 MPa and σ_b of 730 MPa owing to the solution hardening effect of Zr.

Figure 7 shows fracture surfaces of Ti-Nb-Zr-Cr alloys observed by SEM. All the Ti-Nb-Zr-Cr alloys show obvious necking before break. The percentage reduction in area (ψ) after fracture also reflects the plastic deformation ability of materials. It is expressed as:

$$\psi = \frac{(A_0 - A_1)}{A_0} \qquad \text{(Eq 3)}$$

where A_0 is the original cross-sectional area and A_1 is the cross-sectional area after fracture. As shown in Fig. 8, the percentage reduction in area is increased with increase in Zr content, indicating that the local plastic deformation (necking) becomes obvious. According to the stress–strain curves in Fig. 5, Ti-29Nb-4Zr-2Cr and Ti-29Nb-7Zr-2Cr show long working hardening stage, which means that they have large uniform deformation. However, the accumulation of working hardening during tension increases the deformation resistance for local plastic deformation. Thus, they show large elongation but fracture without well-developed necking. Since the working hardening stage is smaller in Ti-29Nb-10Zr-2Cr, the percentage reduction in area becomes a little larger. The work hardening of Ti-29Nb-13Zr-2Cr is weak, so the plasticity is mainly reflected on the obvious necking. Ti-29Nb-13Zr-2Cr performs the largest percentage reduction in area among the four alloys, indicating that it also owns good plasticity. The dimple morphologies observed on the fracture surface (Fig. 7e, f, g and h) show that Ti-29Nb-4Zr-2Cr and Ti-29Nb-7Zr-2Cr have fine and uniform dimples. The dimples are large and deformed in Ti-29Nb-10Zr-2Cr. The amount of deformed dimples is decreased in Ti-29Nb-10Zr-2Cr owing to the great necking. The change of dimples also suggests that local deformation becomes dominant with increased of Zr content. Nevertheless, all the designed Ti-Nb-Zr-Cr alloys can be subjected to cold rolling, perform elongation greater than 18% and show obvious necking, indicating that they all have good plasticity.

4. Discussion

In this study, Ti-29Nb-(4, 7, 10, 13)Zr-2Cr alloys are developed by using 2% Cr to replace 13% Ta in Ti-29Nb-13Ta-4.6Zr. Desirable mechanical properties are obtained by changing Zr content. It is well known that Zr is a neutral element but can reduce the M_s point, so it can be considered as β stabilizer. The present study also indicates that Zr can slightly increase the β stability according to the deformed microstructures (Fig. 4) and the stress–strain curves (Fig. 5). Although the Ti-29Nb-(4, 7, 10, 13)Zr-2Cr alloys all show single β phase in XRD patterns, the β stability strongly influences the mechanical properties owing to the changes of deformation mechanisms. Ti-29Nb-4Zr-2Cr and Ti-29Nb-7Zr-2Cr with metastable β phase show stress-induced martensite transformation and twining deformation, thus they perform the obvious characteristics of nonlinear deformation, low $\sigma_{0.2}$, high ε and large difference between $\sigma_{0.2}$ and σ_b. The characteristics gradually disappear with the increase of β stability. Ti-29Nb-13Zr-2Cr with stable β phase show linear elastic deformation, clear yielding and small difference between $\sigma_{0.2}$ and σ_b. The deceases of ε are mainly attributed to the disappearances of TWIP and TRIP; however, the plasticity is not obviously decreased. Ti-29Nb-13Zr-2Cr performs the largest percentage reduction in area, indicating that local plastic deformation is well developed. Both the $\sigma_{0.2}$ and σ_b are significantly improved by solution hardening of Zr. Usually, the Young's modulus will be also slightly increased by some strengthening effects. However, Zr improves the strength and reduces the Young's modulus in this study by the comprehensive function of stabilizing β phase and increasing the $\overline{B_o}$ value of the alloy.

As biomedical materials, Ti alloys need high strength and low Young's modulus to protect the bone tissue from stress shielding effect. Two parameters are usually used to evaluate the comprehensive mechanical properties. The one is the ratio of tensile strength to Young's modulus (σ_b/E) (Ref 53). The σ_b/E values of C.P.-Ti, Ti-6Al-4V ELI, Ti-15Mo, Ti-29Nb-13Ta-4.6Zr and Ti-35Nb-7Zr-5Ta are 5.29×10^{-3}, 7.95×10^{-3},

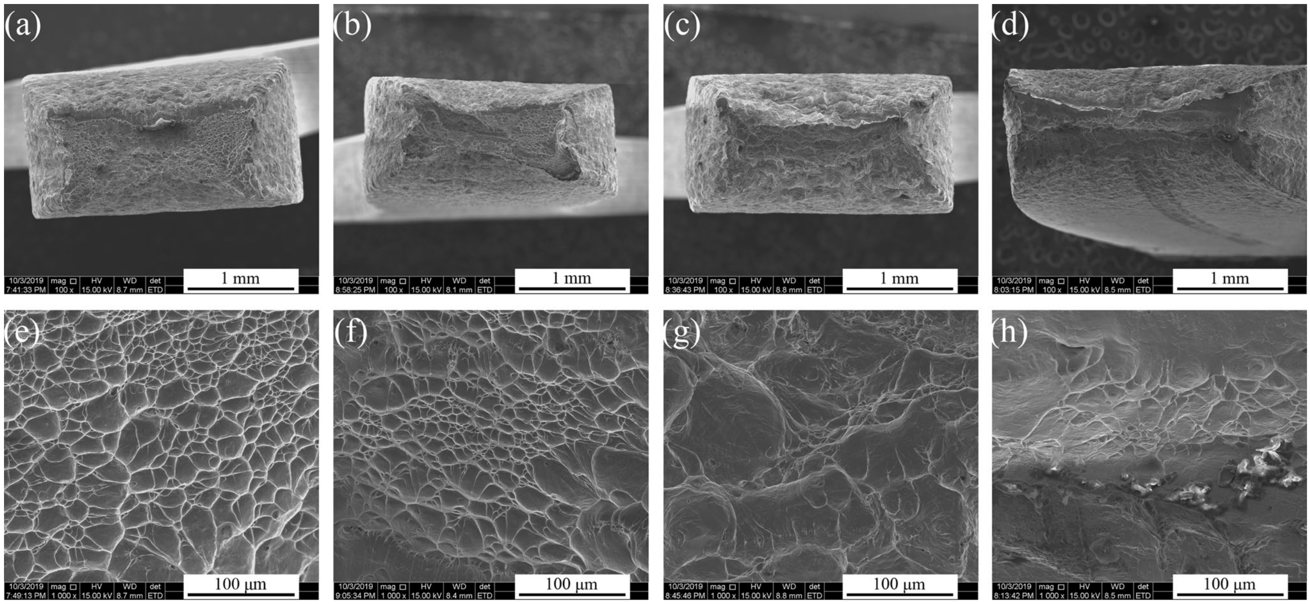

Fig. 7 Fractgraphs (a, b,c and d) and dimple morphologies (e and f) of Ti-Nb-Zr-Cr alloys after tensile tests: (a and e) Ti-29Nb-4Zr-2Cr, (b and f) Ti-29Nb-7Zr-2Cr, (c and g) Ti-29Nb-10Zr-2Cr and (d)(h) Ti-29Nb-13Zr-2Cr

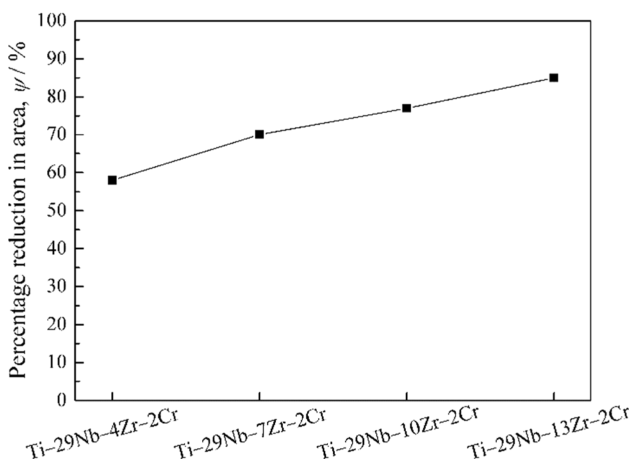

Fig. 8 Percentage reduction in area of Ti-Nb-Zr-Cr alloys after fracture

11.21×10^{-3}, 9.15×10^{-3} and 10.85×10^{-3}, respectively (Ref 4, 5, 45, 54). The Ti-29Nb-4Zr-2Cr with low σ_b and high E present low σ_b/E value of 6.28×10^{-3}. However, the Ti-29Nb-(7, 10, 13)Zr-2Cr alloys present higher σ_b/E values, which are 8.60×10^{-3}, 8.56×10^{-3} and 11.60×10^{-3}, respectively. The other one is elastic energy (δe), which reveals safety performance in use and is expressed as $\delta e = \sigma_{0.2}^2/2E$ (Ref 55). The elastic energies of C.P.-Ti, Ti-6Al-4V ELI, Ti-15Mo, Ti-29Nb-13Ta-4.6Zr and Ti-35Nb-7Zr-5Ta are 1.13, 2.87, 1.90, 1.02 and 2.72 MJ/m^3, respectively (Ref 4, 5, 45, 54). The Ti-29Nb-(4, 7, 10)Zr-2Cr alloys present lower δe values, which are 0.94, 1.34 and 1.69 MJ/m^3, respectively, owing to the lower $\sigma_{0.2}$ and higher E. However, Ti-29Nb-13Zr-2Cr with low E and high $\sigma_{0.2}$ exhibits higher δe value of 4.04 MJ/m^3. Therefore, the Ti-29Nb-13Zr-2Cr alloy performs good comprehensive mechanical properties and is a suitable candidate material for biomedical implants.

5. Conclusions

The following conclusions can be summarized from the above results and discussions:

(1) The Ti-29Nb-(4, 7, 10)Zr-2Cr alloys with metastable β phase show obvious work hardening. The Ti-29Nb-(4, 7)Zr-2Cr alloys perform high elongation due to the twinning-induced plasticity (TWIP) and transformation-induced plasticity (TRIP) during tension.

(2) The addition of Zr slightly increases lattice parameter, provides solution strengthening effect and enhances the β stability of the Ti-29Nb-(4, 7, 10, 13)Zr-2Cr alloys. With the increase in Zr content, the Young's modulus shows a gradually decreasing trend because the $\overline{B_o}$ value of the alloy is increased by adding Zr.

(3) The Ti-29Nb-13Zr-2Cr alloy performs high yield strength of 713 MPa, elongation of 18% and low Young's modulus of 63GPa and is a promising candidate for biomedical applications.

Acknowledgments

This work was partially supported by the Natural Science Foundation of Shanghai, China (No. 15ZR1428400), "The Belt and Road" international cooperation project of Shanghai Science and Technology Committee (No. 19510744700), the project of Creation of Life Innovation Materials for Interdisciplinary and International Researcher Development, Tohoku University, Japan sponsored by Ministry, Education, Culture, Sports, Science and Technology, Japan, and the Grant-in Aid for Scientific Research (B) (No. 17H03419) from Japan Society for the Promotion of Science (JSPS), Tokyo, Japan.

References

1. Q.Z. Chen and G.A. Chen, Metallic implant Biomaterials, *Mater. Sci. Eng. R*, 2015, **87**, p 1–57
2. F.A. Shah, M. Trobos, P. Thomsen, and A. Palmquist, Commercially Pure Titanium (cp-Ti) Versus Titanium Alloy (Ti6Al4V) Materials as Bone Anchored Implants—is One Truly Better than the Other?, *Mater. Sci. Eng. C*, 2016, **62**, p 960–966
3. M. Niinomi, Recent Metallic Materials for Biomedical Applications, *Met. Mat. Trans. A*, 2002, **33A**, p 477–486
4. M. Niinomi, M. Nakai, and J. Hieda, Development of new Metallic Alloys for Biomedical Applications, *Acta Biomater.*, 2012, **8**, p 3888–3903
5. M. Long and H.J. Rack, Titanium Alloys in Total Joint Replacement—A Materials Science Perspective, *Biomaterials*, 1998, **19**, p 1621–1639
6. M. Niinomi, Recent Research and Development in Titanium Alloys for Biomedical Applications and Healthcare Goods, *Sci. Technol. Adv. Mater.*, 2003, **4**, p 445–454
7. L.C. Zhang and L.Y. Chen, A Review on Biomedical Titanium Alloys: Recent Progress and Prospect, *Adv. Eng. Mater.*, 2019, **21**, p 1–29
8. M. Abdel-Hady, H. Fuwa, K. Hinoshita, H. Kimura, Y. Shinzato, and M. Morinaga, Phase Stability Change with Zr Content in β-type Ti-Nb Alloys, *Scr. Mater.*, 2007, **57**, p 1000–1003
9. A. Mishra, J.A. Davidson, R. Poggie, P. Kovacs, and T.J. Fitzgerald, Mechanical and Tribological Properties and Biocompatibility of diffusion Hardened Ti-13Nb-13Zr—A New Titanium Alloy for Surgical Implants, *ASTM STP*, 1996, **1272**, p 96–116
10. M. Lai, Y. Gao, B. Yuan, and M. Zhu, Effect of Pore Structure Regulation on the Properties of Porous TiNbZr Shape Memory Alloys for Biomedical Application, *J. Mater. Eng. Perform.*, 2015, **24**, p 136–142
11. S. Ozan, J.X. Lin, Y.C. Li, Y.W. Zhang, K. Munir, H.W. Jiang, and C. Wen, Deformation Mechanism and Mechanical Properties of a Thermomechanically Processed β Ti-28Nb-35.4Zr Alloy, *J. Mech. Behav. Biomed. Mater*, 2018, **78**, p 224–234
12. Q. Li, M. Niinomi, M. Nakai, Z.D. Cui, S.L. Zhu, and X.J. Yang, Effect of Zr on Super-Elasticity and Mechanical Properties of Ti-24 at% Nb-(0, 2, 4) at% Zr Alloy Subjected to Aging Treatment, *Mater. Sci. Eng., A*, 2012, **536**, p 197–206
13. C.D. Rabadia, Y.J. Liu, G.H. Cao, Y.H. Li, C.W. Zhang, T.B. Sercombe, H. Sun, and L.C. Zhang, High-Strength β Stabilized Ti-Nb-Fe-Cr Alloys with Large Plasticity, *Mater. Sci. Eng., A*, 2018, **732**, p 368–377
14. A.B. Elshalakany, S. Ali, A.A. Mata, A.K. Eessaa, P. Mohan, T.A. Osman, and V.A. Borrás, Microstructure and Mechanical Properties of Ti-Mo-Zr-Cr Biomedical Alloys by Powder Metallurgy, *J. Mater. Eng. Perform.*, 2017, **26**, p 1262–1271
15. M. Nakai, M. Niinomi, X.F. Zhao, and X.L. Zhao, Self-adjustment of Young's Modulus in Biomedical Titanium Alloys During Orthopaedic Operation, *Mater. Letters.*, 2011, **65**, p 688–690
16. Q. Li, G.H. Ma, J.J. Li, M. Niinomi, M. Nakai, Y. Koizumi, D.X. Wei, T. Kakeshita, T. Nakano, A. Chiba, X.Y. Liu, K. Zhou, and D. Pan, Development of Low-Young's Modulus Ti-Nb-Based Alloys with Cr Addition, *J. Mater. Sci.*, 2019, **54**, p 8675–8683
17. C.D. Rabadia, Y.J. Liu, L.Y. Chen, S.F. Jawed, L.Q. Wang, H. Sun, and L.C. Zhang, Deformation and Strength Characteristics of Laves Phases in Titanium Alloys, *Mater. Des.*, 2019, **179**, p 1–9
18. M. Nakal, M. Niinomi, and T. Oneda, Improvement in Fatigue Strength of Biomedical β-type Ti-Nb-Ta-Zr Alloy While Maintaining Low Young's Modulus Through Optimizing ω-Phase Precipitation, *Metall. Mater. Trans. A*, 2012, **43A**, p 294–302
19. N. Hafeez, S.F. Liu, E. Lu, L.Q. Wang, R. Liu, W.J. Lu, and L.C. Zhang, Mechanical Behavior and Phase Transformation of β-Type Ti-35Nb-2Ta-3Zr Alloy Fabricated by 3D-PRINTING, *J. Alloys Compd.*, 2019, **790**, p 117–126
20. L.C. Zhang, L.Y. Chen, and L.Q. Wang, Surface Modification of Titanium and Titanium Alloys: Technologies, Developments, and Future Interests, *Adv. Eng. Mater.*, 2020, **22**, p 1–37
21. L. Pawlowski, Finely Grained Nanometric and Submicrometric Coatings by Thermal Spraying: A Review, *Surf. Coat. Technol.*, 2008, **202**, p 4318–4328
22. P. Favia and R. d'Agostino, Plasma Treatments and Plasma Deposition of Polymers for Biomedical Applications, *Surf. Coat. Technol.*, 1998, **98**, p 1102–1106
23. H. Lee, S. Mall, and W.Y. Allen, Fretting Fatigue Behavior of Shot-Peened Ti-6Al-4V Under Seawater Environment, *Mater. Sci. Eng., A*, 2006, **420**, p 72–78
24. T. Fu, Z. Zhan, L. Zhang, Y. Yang, Z. Liu, J. Liu, L. Li, and X. Yu, Effect of Surface Mechanical Attrition Treatment on Corrosion Resistance of Commercial Pure Titanium, *Surf. Coat. Technol.*, 2015, **280**, p 129–135
25. L.Q. Wang, L.C. Xie, Y.T. Lv, L.C. Zhang, L.Y. Chen, Q. Meng, J. Qu, D. Zhang, and W.J. Lu, Microstructure Evolution and Superelastic Behavior in Ti-35Nb-2Ta-3Zr Alloy Processed by Friction Stir Processing, *Acta Mater.*, 2017, **131**, p 499–510
26. D. Kuroda, M. Niinomi, M. Morinaga, Y. Kato, and T. Yashiro, Design and Mechanical Properties of New β Type Titanium Alloys for Implant Materials, *Mater. Sci. Eng., A*, 1998, **243**, p 244–249
27. M. Niinomi, T. Hattori, K. Morikawa, T. Kasuga, A. Suzuki, H. Fukui, and S. Niwa, Development of Low Rigidity β-type Titanium Alloy for Biomedical Applications, *Mater. Trans.*, 2002, **43**, p 2970–2977
28. N. Sumitomo, K. Noritake, T. Hattori, K. Morikawa, S. Niwa, K. Sato, and M. Niinomi, Experiment Study on Fracture Fixation with Low Rigidity Titanium Alloy, *J. Mater. Sci.: Mater. Med.*, 2008, **19**, p 1581–1586
29. R.P. Kolli, W.J. Joost, and S. Ankem, Phase Stability and Stress-Induced Transformations in Beta Titanium Alloys, *JOM*, 2015, **67**, p 1273–1280
30. Y.L. Hao, M. Niinomi, D. Kuroda, K. Fukunaga, Y.L. Zhou, R. Yang, and A. Suzuki, Young's Modulus and Mechanical Properties of Ti-29Nb-13Ta-4.6Zr in Relation to α'' Martensite, *Metall. Mater. Trans. A*, 2002, **33A**, p 31–37
31. Y. Zhou, Y.X. Li, X.J. Yang, Z.D. Cui, and S.L. Zhu, Influence of Zr Content on Phase Transformation, Microstructure and Mechanical Properties of Ti75-*x*Nb25Zr*x* (x = 0-6) Alloys, *J. Alloys Compd.*, 2009, **486**, p 628–632
32. J. Málek, F. Hnilica, J. Veselý, B. Smola, K. Kolařík, J. Fojt, M. Vlach, and V. Kodetová, The Effect of Zr on the Microstructure and Properties of Ti-35Nb-XZr Alloy, *Mater. Sci. Eng., A*, 2016, **675**, p 1–10
33. M.J. Lai, T. Li, and D. Raabe, ω Phase Acts as a Switch Between Dislocation Channeling and Joint Twinning- and Transformation-Induced Plasticity in a Metastable β Titanium Alloy, *Acta Mater.*, 2018, **151**, p 67–77
34. H. Tobe, H.Y. Kim, T. Inamura, H. Hosoda, and S. Miyazaki, Origin of 332 Twinning in Metastable β-Ti Alloys, *Acta Mater.*, 2014, **64**, p 345–355
35. Y. Mantani, Y. Takemoto, M. Hida, and A. Sakakibara, Formation of a″ Martensite and {332}⟨113⟩Twin During Tensile Deformation in Ti-40 mass%Nb Alloy, *J. JPN. I. MET.*, 2002, **10**, p 1022–1029
36. Y. Takemoto, M. Hida, and A. Sakakibara, Martensitic, 332⟨113⟩Twin in β Type Ti-Mo Alloy, *J. JPN. I. MET.*, 1996, **60**, p 1072–1078
37. X.H. Min, S. Emura, T. Nishimura, K. Tsuchiya, and K. Tsuzaki, Microstructure, Tensile Deformation Mode and Crevice Corrosion Resistance in Ti-10Mo-xFe Alloys, *Mater. Sci. Eng., A*, 2010, **527**, p 5499–5506
38. Q. Li, P. Miao, J.J. Li, M.F. He, M. Nakai, M. Niinomi, A. Chiba, T. Nakano, X.Y. Liu, K. Zhou, and D. Pan, Effect of Nb Content on Microstructures and Mechanical Properties of Ti-xNb-2Fe Alloys, *J. Mater. Eng. Perform.*, 2019, **16**, p 5501–5508
39. M.J. Lai, C.C. Tasan, and D. Raabe, On the Mechanism of 332 Twinning in Metastable β Titanium Alloys, *Acta Mater.*, 2016, **111**, p 173–186
40. X.H. Min, X.J. Chen, S. Emura, and K. Tsuchiya, Mechanism of Twinning-Induced Plasticity in β-type Ti-15Mo Alloy, *Scr. Mater.*, 2013, **69**, p 393–396
41. M. Niinomi, T. Akahori, and M. Nakai, In situ X-ray Analysis of Mechanism of Nonlinear Super Elastic Behavior of Ti-Nb-Ta-Zr System Beta-Type Titanium Alloy for Biomedical Applications, *Mater. Sci. Eng., C*, 2008, **28**, p 406–413
42. X. Jin, S. Emura, X.H. Min, and K. Tsuchiya, Strain-Rate Effect on Work-Hardening Behavior in β-type Ti-10Mo-1FE alloy with TWIP effect, *MATER. Sci. Eng., A*, 2017, **707**, p 701–707
43. M. Abdel-Hady, K. Hinoshita, and M. Morinaga, General Approach to Phase Stability and Elastic Properties of β-type Ti-Alloys Using Electronic Parameters, *Scr. Mater.*, 2006, **55**, p 477–480

44. J. Chen, F.C. Ma, P. Liu, C.H. Wang, X.K. Liu, W. Li, and Q.Y. Han, Effects of Nb on Superelasticity and Low Modulus Properties of Metastable β-Type Ti-Nb-Ta-Zr Biomedical Alloys, *J. Mater. Eng. Perform.*, 2019, **28**, p 1410–1418
45. Y.H. Li, C. Yang, H.D. Zhao, S.G. Qu, X.Q. Li, and Y.Y. Li, New Developments of Ti-Based Alloys for Biomedical Applications, *Mater.*, 2014, **7**, p 1709–1800
46. Y.L. Hao, S.J. Li, S.Y. Sun, C.Y. Zheng, and R. Yang, Elastic Deformation Behaviour of Ti-24Nb-4Zr-7.9Sn for Biomedical Applications, *Acta Biomater*, 2007, **3**, p 277–286
47. T. Ahmed, M. Long, J. Silvestri, C. Ruiz, and H. Rack, A New Low Modulus, Biocompatible Titanium Alloy, *Titanium'95 Science and Technology UK*, 1996, **II**, p 1760–1767
48. J.H. Gao, Y.H. Huang, D.K. Guan, A.J. Knowles, L. Ma, D. Dye, and W.M. Rainforth, Deformation Mechanisms in a Metastable Beta Titanium Twinning Induced Plasticity Alloy with High Yield Strength and High Strain Hardening Rate, *Acta Mater.*, 2018, **152**, p 301–314
49. M. Marteleur, F. Sun, T. Gloriant, P. Vermaut, P.J. Jacques, and F. Prima, On the Design of New β-Metastable Titanium Alloys with Improved Work Hardening Rate Thanks to Simultaneous TRIP and TWIP effects, *Scr. Mater.*, 2012, **66**, p 749–752
50. C. Liu, J.Q. Qin, Z.H. Feng, S.L. Zhang, M.Z. Ma, X.Y. Zhang, and R.P. Liu, Improving the Microstructure and Mechanical Properties of Zr-Ti Alloy by Nickel Addition, *J. Alloys Compd.*, 2018, **737**, p 405–411
51. C.D. Rabadia, Y.J. Liu, S.F. Jawed, L. Wang, Y.H. Li, X.H. Zhang, T.B. Sercombe, H. Sun, and L.C. Zhang, Improved Deformation Behavior in Ti-Zr-Fe-Mn Alloys Comprising the C14 Type Laves and β Phases, *Mater. Des.*, 2018, **160**, p 1059–1070
52. L.Y. Du, L. Wang, W. Zhai, L. Hu, J.M. Liu, and B. Wei, Liquid State Property, Structural Evolution and Mechanical Behavior of Ti-Fe Alloy Solidified Under Electrostatic Levitation Condition, *Mater. Des.*, 2018, **160**, p 48–57
53. H. Matsumoto, S. Watanabe, and S. Hanada, Microstructures and Mechanical Properties of Metastable TiNbSn Alloys Cold Rolled and Heat Treated, *J. Alloys Compd.*, 2007, **439**, p 146–155
54. M. Niinomi, Mechanical Properties of Biomedical Titanium Alloys, *Mater. Sci. Eng., A*, 1998, **243**, p 231–236
55. Y.Z. Zhan, C.L. Li, and W.P. Jiang, β-type Ti-10Mo-1.25Si-*x*Zr Biomaterials for Applications in Hard Tissue Replacements, *Mater. Sci. Eng. C*, 2012, **32**, p 1664–1668